Evidence of carrier mediated room temperature ferromagnetism in transparent semiconducting $Sn_{1-x}Co_xO_{2-\delta}$ thin films

Evidence of carrier mediated room temperature ferromagnetism in transparent semiconducting $Sn_{1-x}Co_xO_{2-\delta}$ thin films

K Gopinadhan, Subhash C Kashyap, Dinesh K Pandya and Sujeet Chaudhary

Thin Film Laboratory, Department of Physics, Indian Institute of Technology Delhi, New Delhi-110016, India

E-mail: skashyap@physics.iitd.ac.in

Abstract
Magnetic ordering in Co-substituted spray pyrolyzed SnO_2 thin films has been investigated by magneto-transport studies of $Sn_{1-x}Co_xO_{2-\delta}$ and F co-doped films. The free carrier concentration and room temperature ferromagnetism induced in $Sn_{1-x}Co_xO_{2-\delta}$ thin films with cobalt concentrations up to $x = 0.10$ are found to be closely related to each other. Both the carrier concentration and the saturation magnetic moment increase monotonically with the concentration of Co, and attain maximum values of 2.2×10^{19} cm^{-3} and 0.26 μ_B/Co-ion, respectively, at $x = 0.10$. The substitution of O^{2-} with F^- (nearly 10 atomic percent (a/o)) has resulted in much higher values of both carrier concentration (2.07×10^{20} cm^{-3}) and magnetic moment (0.80 μ_B/Co-ion). Also, anomalous behavior of the Hall effect has been observed. The carrier mediated interaction is proposed to be the most probable mechanism responsible for ferromagnetism in these films. The temperature dependence of the magnetization of these films predicts a Curie temperature exceeding 573 K. All the films are optically transparent ($>75\%$) in the visible spectral region.

1. Introduction

Inducing order in the spin of the charge carriers in a conventional wide band gap semiconductor and thereby getting room temperature ferromagnetism (RTFM) is an ongoing challenge in realizing semiconductor based spintronic devices. Ferromagnetic oxide semiconductors have actively been investigated both theoretically and experimentally for the last few years, and RTFM has been reported in samples of TiO_2 [1–5], ZnO [6–9], CuO [10], In_2O_3 [11–14], SnO_2 [15–19] etc with incorporated transition metals (TM).

Owing to its high optical transparency and tunable semiconductivity, tin oxide doped with transition elements could be a potential material for multifunctional spintronic devices. Attempts have therefore been made to induce and investigate RTFM in doped tin oxide thin films. However, the issue related to the origin of ferromagnetism in this material

is still under debate. So far, the study of rutile $Sn_{1-x}Co_xO_{2-\delta}$ thin films [15] suggests that: (i) the Curie temperature (T_C) is well above room temperature (RT), and (ii) films with $x = 0.05$ possess a maximum magnetic moment of $\sim$7.8 μ_B/Co-ion that is metastable in origin. Studies of $Sn_{1-x}Co_xO_{2-\delta}$ bulk samples suggest: (i) a magnetic moment (m) of $\sim$0.133 μ_B/Co [17] and (ii) the absence of ferromagnetic ordering [16]. A recent theoretical study by Wang *et al* [20] predicted the presence of high temperature ferromagnetism in Co-doped SnO_2, and that the ferromagnetism could be stabilized by increasing the density of n-type carriers. We have undertaken a detailed study of $Sn_{1-x}Co_xO_{2-\delta}$ ($0 \leqslant x \leqslant 0.15$) thin films, with a view to enhancing and stabilizing the RTFM via possible increase in the free carrier concentration by additionally doping with F. This report forms the first such attempt for the F, Co:SnO_2 system containing a concentration of free electrons of as much as $\sim$2 $\times$ 10^{20} cm^{-3}. The analyses of the observed electrical and

magnetic properties of $Sn_{1-x}Co_xO_{2-\delta-y}F_y$ thin films (with x varying up to 0.15 and F-dopant concentration y upto 0.10) clearly establishes a relation between the carrier concentration and magnetic moment in $Sn_{1-x}Co_xO_{2-\delta-y}$ thin films, in which δ and hence the free carrier concentration is controlled by F-doping. Our F-doped results, possibly reported for the first time, provide strong support for the carrier-induced exchange interaction being responsible for ferromagnetic ordering in the $Sn_{1-x}Co_xO_{2-\delta}$ semiconductor system.

2. Experimental details

Thin films of both cobalt-doped SnO_2 and fluorine and cobalt co-doped SnO_2 were deposited by a sequential spray pyrolysis technique (in three steps). These spray depositions were carried out in an ambient atmosphere using nitrogen as the carrier gas at a pressure of $\sim 4 \times 10^4$ N m^{-2}. The aqueous solutions of ($SnCl_4.5H_2O$ (1 M), NH_4F (1 M)) and $(CH_3COO)_2Co.4H_2O$ (0.1 M) were atomized on highly pure (non-magnetic) quartz substrates maintained at 450 °C. Appropriate volumes of the two solutions of the constituents (Sn and Co) were taken so as to vary the concentration of cobalt in $Sn_{1-x}Co_xO_{2-\delta}$ samples from $x = 0.025$ to 0.15 in steps of 0.025. In the first stage of spray pyrolysis, half of the $SnCl_4.5H_2O$ solution was sprayed (in the case of fluorine doping, half of the mixture of $SnCl_4.5H_2O$ and NH_4F solutions was sprayed). In the second step, after waiting for about 10 min, the entire volume of the $(CH_3COO)_2Co.4H_2O$ solution was sprayed. Following this, after a wait of about 30 min, the remaining half of the $SnCl_4.5H_2O$ solution was finally sprayed as the third step. Each spray lasted for about 25 s. Following the third step, the deposited film was kept at 500 °C for another 30 min, to allow diffusion of Co-ions into the SnO_2 matrix. The deposition parameters were optimized to yield good quality films exhibiting thermally stable magnetism and to minimize the presence of Cl in the films [19, 21]. The samples were characterized for their structural, electrical and magnetic properties by employing various techniques similar to that used in Mn-doped SnO_2 thin films [19].

3. Results and discussion

Figure 1(a) shows the glancing angle x-ray diffractograms (GAXRD) of the spray pyrolyzed $Sn_{1-x}Co_xO_{2-\delta}$ thin films with $x = 0$, 0.05, 0.10 and 0.15 (data exist for other films having different concentration of Co, but have not been shown for brevity) and of Co_3O_4 thin film. The latter was deposited by spray pyrolysis of cobalt acetate solution. The XRD peaks were identified using a second derivative method which uses a sliding polynomial filter and allows an accurate detection of low intensity peaks overlapping with the high intensity peaks. The measured XRD peaks were fitted by pseudo-Voigt functions in order to determine the position, intensity and broadening of the peaks. As is evident from figure 1(a), the diffractogram corresponding to pure SnO_2 thin film shows strong peaks corresponding to the rutile-type cassiterite (tetragonal) phase [22]. None of the peaks corresponding to either orthorhombic SnO,
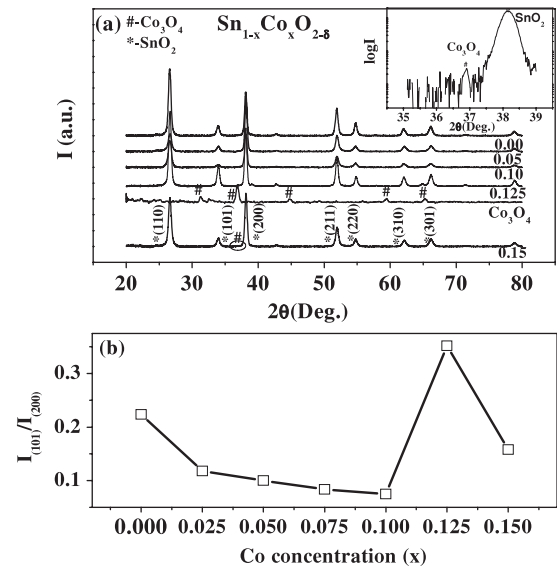
Figure 1. (a) X-ray diffraction patterns of the $Sn_{1-x}Co_xO_{2-\delta}$ thin films with $x = 0.00$, 0.05, 0.10 and 0.15 and pure Co_3O_4 thin film. The inset shows the logarithmic intensity plot of $Sn_{0.85}Co_{0.15}O_{2-\delta}$ showing a small peak of Co_3O_4 secondary phase. (b) Variation of the intensity ratio $I_{(101)}/I_{(200)}$ of the XRD peaks with x, indicating the incorporation of Co in SnO_2.

cobalt metal, cobalt oxides or any binary Sn–Co phase are observed in the diffractograms of any of the Co-substituted tin oxide films for $x \leqslant 0.125$. This suggests that the added cobalt neither segregates nor forms any crystalline impurity phase (within the detectable limits). However, the presence of a very small quantity of any nano-sized impurities can be completely ruled out by further investigations based on complementary analytical techniques such as cross-sectional transmission electron microscopy combined with electron energy loss spectroscopy.

Since all the peaks in the x-ray diffractogram of the Co-doped SnO_2 films correspond to the known peaks of the tetragonal phase of SnO_2, the $Sn_{1-x}Co_xO_{2-\delta}$ films for $x \leqslant 0.125$ are single phase. At $x = 0.15$, an additional low intensity peak of Co_3O_4 appears (clearly seen in the inset to figure 1) which implies that the solid solubility of Co in SnO_2 thin films seems to be limited to $x < 0.15$. It may be noted that the solubility limit of Co in the present case is, however, lower than the reported value of $x = 0.27$ for pulsed laser deposited SnO_2 films [15] but higher than the cited value of $x \leqslant 0.08$ for powder samples [17]. This variation in the solubility limit can be understood as the thin film processes, being atomistic and occurring under non-equilibrium conditions, can lead to the incorporation of much larger quantities of additive in the films than bulk, depending upon the film growth techniques/conditions.

In order to calculate the lattice parameters from the recorded GAXRD, (110), (101), (200), (211) and (220) reflections appearing at lower 2θ values (and thus less affected by the $\kappa_{\alpha 1}$ and $\kappa_{\alpha 2}$ splitting of the incident beam) have been employed. The lattice parameters of a cobalt-free SnO_2 thin film are estimated to be $a = 4.737$ Å and $c = 3.186$ Å, which is in agreement with the reported result [22]. With the addition

of cobalt, the lattice constant '*a*' shows a 0.2% decrease on increasing *x* up to 0.10, whereas the lattice parameter '*c*' remains unaffected. These results are in agreement with the fact that the difference in the ionic radius of Co^{2+} (0.65 Å) and Sn^{4+} (0.69 Å) for an octahedral coordination [23] is rather small, leading to very small changes in the lattice constants on doping with Co.

To see the effect of Co-substitution on the intensities of SnO_2 peaks, detailed analysis of the XRD data has been carried out. The exact integrated peak intensities have been calculated after stripping $\kappa_{\alpha 2}$ peaks using the Rachinger method [24] and performing the background correction. It is found that as the Co-concentration is increased from $x = 0$ to 0.10, the ratio of the intensities of the (101) to (200) peak decreases from 0.221 to 0.076 (see figure 1(b)) while the intensity of x-rays diffracted from other planes is not affected much (as determined by the texture coefficients). This indicates the preferential growth of Co–doped SnO_2 films under the above mentioned processing conditions. The observed decrease in the intensity ratio $I_{(101)}/I_{(200)}$ up to $x = 0.10$ is ascribed to the substitution of Sn by Co in the lattice of SnO_2. It is emphasized here that the atomic scattering factor for Co is almost half the value for Sn, since the atomic number of Co is 27 as against a value of 50 for Sn. Therefore, any substitution of Sn by Co changes the structure factor of the lattice which, in turn, is reflected in the change in the XRD peak intensities on Co-substitution. This systematic evolution of the (101) and (200) peaks of SnO_2 with increase in Co-concentration is therefore linked with the incorporation of Co into the SnO_2 matrix. The increase in the intensity ratio, $I_{(101)}/I_{(200)}$, above a Co-concentration of 10 atomic percent (a/o) is possibly due to the crossover from substitutional to interstitial site incorporation of Co in the SnO_2 lattice as this would enhance the structure factor and hence the intensity. Also, this inference of interstitial occupation stems from the reported result [25] that the size of the interstitial sites in the SnO_2 lattice is comparable to the ionic size of the magnetic dopant (Co) and therefore, energy wise, interstitial occupation is also a possibility. It may be pointed out that powder x-ray diffraction may be detecting the presence of secondary phase/s, and additional research study by a complementary technique such as cross-sectional transmission electron microscopy combined with electron energy loss spectroscopy may be needed to completely eliminate the possibility of the formation of secondary phase/s.

A bare quartz substrate (without the SnO_2 film) was treated at the same temperature of 450 °C and annealed at 500 °C. The magnetization (*M*) versus applied magnetic field (*H*) behavior of this substrate shows a diamagnetic relationship, indicating that there are no detectable ferromagnetic impurities present in the quartz substrate. Further, the *M*–*H* behavior of undoped SnO_2 film has also been studied, which indicates a diamagnetic relationship in agreement with the literature. We show in figures 2(a)–(c), the *M*–*H* behavior of three films of $Sn_{1-x}Co_xO_{2-\delta}$, with *x* = 0.025, 0.10 and 0.125, respectively, at room temperature (RT). Although, *M*–*H* data exist for other films with *x* = 0, 0.050, 0.075, and 0.150 as well, these have not been included for the sake of brevity. The magnetization
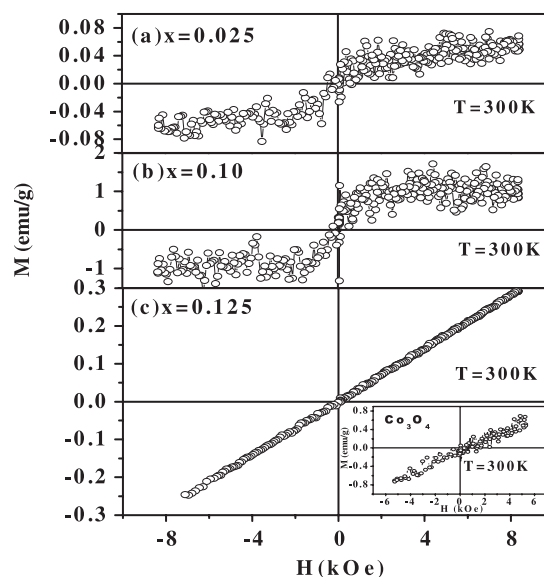
Figure 2. *M* versus *H* behavior of $Sn_{1-x}Co_xO_{2-\delta}$ thin films with different cobalt concentrations: (a) 2.5 a/o, (b) 10 a/o and (c) 12.5 a/o. The inset in (c) shows the paramagnetic *M* versus *H* behavior of Co_3O_4 thin film. All the *M*–*H* plots were recorded at RT.

data have been corrected for the diamagnetic contribution from the quartz substrate and the sample holder. While the $Sn_{1-x}Co_xO_{2-\delta}$ thin film with the smallest Co-concentration of $x = 0.025$ exhibited very weak ferromagnetic behavior in its *M*–*H* plot, the films with $x = 0.050$, 0.075 and 0.100 showed room temperature soft ferromagnet-like behavior. The saturation magnetization in the Co-substituted films is optimized with incorporation of cobalt (i.e. *x*), reaching a maximum value of 0.26 μ_B/Co-ion and a coercivity of 40 Oe for $x = 0.10$ as seen in figure 3(b). However, as *x* is increased to 0.125 and beyond, it is observed that the ferromagnetism suddenly disappears. Both the films with $x = 0.125$ and 0.150 exhibit paramagnetic behavior at RT. It may be recalled that the XRD analysis of the films with cobalt concentration up to $x = 0.125$ does not reveal any trace of cobalt or oxides of cobalt, and the one with $x = 0.15$ revealed the presence of Co_3O_4. To the best of our knowledge, none of the alloys of Sn, Co and O is ferromagnetic at room temperature. To further ensure the absence of any ferromagnetic impurities in the starting precursors, pure cobalt acetate was also spray decomposed at the same temperature of 450 °C (as in the case of $Sn_{1-x}Co_xO_{2-\delta}$ film deposition) on the quartz substrate. The *M*–*H* curve of the resulting pure Co_3O_4 (as confirmed from its XRD analysis) film showed a paramagnetic behavior (the inset of figure 2(c)). This is consistent with the reported paramagnetic behavior of Co_3O_4 at RT [26]. Since the films have been prepared under ambient conditions at 450 °C, the possibility of the formation of metallic Co clusters is practically non-existent. This has been further supported by the sudden disappearance of ferromagnetism at higher cobalt concentrations ($x \geqslant 0.10$). From the foregoing, we tend to believe that the ferromagnetism is a result of a magnetic interaction arising due to change in the electronic structure caused by the incorporation of Co-ions into the SnO_2 lattice.
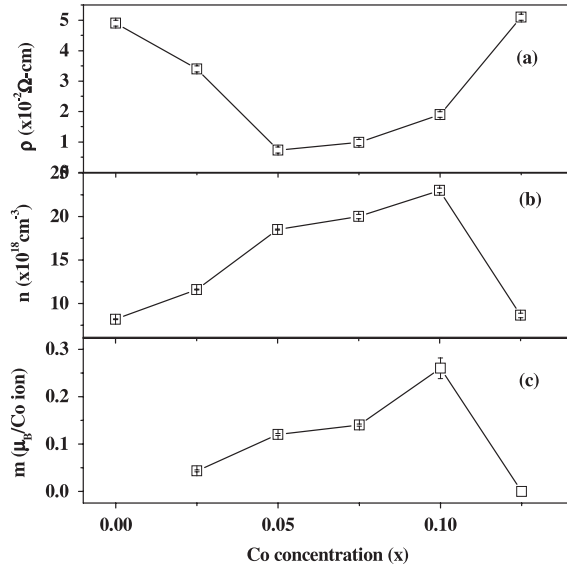
Figure 3. Dependence of (a) electrical resistivity ρ, (b) free carrier concentration n and (c) saturation magnetic moment m (in μ_B/Co-ion)at RT of the $Sn_{1-x}Co_xO_{2-\delta}$ thin films on the Co-concentration, x.

Figure 4. Hall resistivity ρ_{xy} versus applied field H for the $Sn_{0.90}Co_{0.10}O_{2-\delta}$ sample showing the anomalous behavior at RT. The anomalous term can be separated from the ordinary Hall effect (refer to text for details). The inset shows the anomalous contribution.

To further investigate the likely exchange mechanism responsible for the observed ferromagnetic ordering in the $Sn_{1-x}Co_xO_{2-\delta}$ films, we have measured their electrical resistivity and estimated free carrier concentration (n) from Hall measurements at room temperature. As shown in figure 3(a), the electrical resistivity of the $Sn_{1-x}Co_xO_{2-\delta}$ films was found to be dependent on x. The resistivity of these films, however, did not show any monotonic variation with Co-concentration, which could possibly be ascribed to both the variation in carrier concentration and mobility. The dependence of the carrier concentration, n, in the $Sn_{1-x}Co_xO_{2-\delta}$ films with cobalt concentration, x, as estimated from the Hall measurements at higher magnetic field is shown in figure 3(b). This measurement confirmed that electrons are the majority carriers in the spray pyrolyzed Co-doped SnO_2 films. One can note that both the magnetic moment (figure 3(c)) and the carrier concentration (figure 3(b)) are found to increase with the increase in concentration of cobalt in the range of $x = 0.025$–0.10 over which the films are ferromagnetic at RT. The observed increase in carrier concentration on Co-substitution is expected to be a result of the formation of a solid solution between SnO_2 and Co_3O_4, which populates oxygen vacancies when Sn^{4+} is substituted by Co^{2+} in the SnO_2 lattice. It may be noted that with increase in Co-concentration from $x = 0.05$ to 0.10, the average grain size decreases from 23 to 21 nm (as calculated from the broadening of the XRD peaks at lower angular values), which then enhances grain boundary scattering and thus reduces the mobility, counteracting the enhancement in carrier concentration and thus leading to slight increase in resistivity. Further increase in cobalt concentration, however, neither enhances carrier concentration nor results in any FM ordering in these films. Possibly, at these higher concentrations ($x > 0.10$), Co prefers to go interstitially rather than substitutionally.
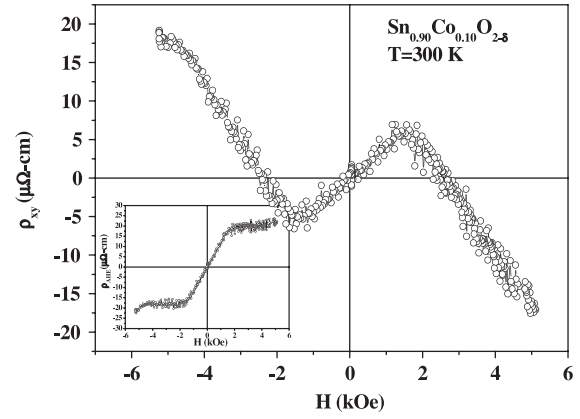
As seen clearly from figures 1(b), 3(b) and (c) the three quantities, i.e. the $I_{(101)}/I_{(200)}$ ratio, the carrier concentration and the saturation magnetic moment, which are caused by the structural, electronic and magnetic changes respectively, exhibit qualitatively similar variation with increase in Co-concentration in SnO_2 films. These results clearly demonstrate the one-to-one relationship between the RTFM and the extra free carriers induced due to addition of Co in SnO_2.

The Hall resistivity ρ_{xy} in magnetic materials can be expressed as

$$\rho_{xy} = R_0 B + \mu_0 R_{AHE} M.$$

The first term is due to the ordinary Hall effect and the second is due to the anomalous Hall effect (AHE), where B is the magnetic induction, M the magnetization and R_{AHE} the anomalous Hall coefficient. Note that $R_{AHE}(T) = \alpha \rho_{xx}(0, T)$, where $\rho_{xx}(0, T)$ is the normal resistivity at zero field and α is a T-independent parameter with the dimension of mobility. We have observed an anomalous behavior in the Hall resistivity (figure 4) of the sample $Sn_{0.90}Co_{0.10}O_{2-\delta}$ at lower magnetic fields. The observation of the AHE is indicative of the spin polarization of the carriers where it mediates the ferromagnetic interaction. It is worth mentioning here that the observation of AHE can also occur if magnetic particles are suspended in a semiconducting matrix as in the case of Co clusters embedded in a TiO_2 matrix [27]. But the temperature dependence of the magnetization observed in our case (as would be discussed later in the paper), the saturation of the Hall resistivity and the magnetization at the same applied magnetic field (see inset of figure 4), indeed proved that this is not the case, i.e. there is no Co cluster formation.
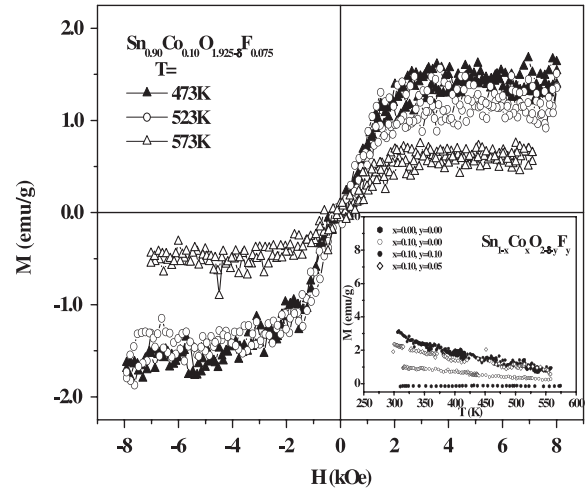
To look into the possibility of carrier mediated ferromagnetic interaction further, the sample with the highest magnetic moment, i.e. $Sn_{0.90}Co_{0.10}O_{2-\delta}$, has been co-doped with different doping levels of fluorine to purposely further increase the free electron concentration. It is well known that the free electron concentration in SnO_2 can be increased either by doping it with Sb or with F [28–30]. Three samples of
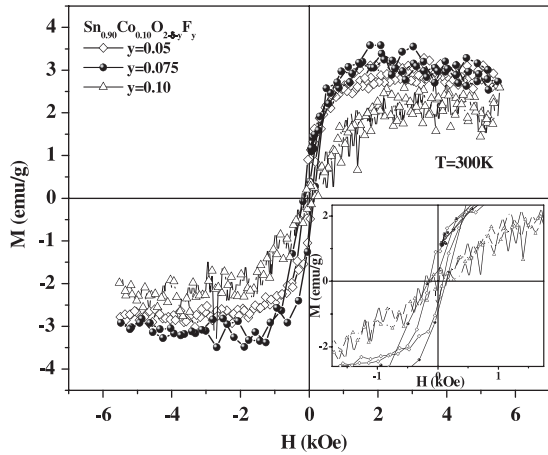
Figure 5. *M* versus *H* behavior of F-doped $Sn_{0.90}Co_{0.10}O_{2-\delta}$ thin films at RT with different fluorine concentrations: (a) 5 a/o, (b) 7.5 a/o and (c) 10 a/o. The data for 7.5 a/o has still some diamagnetic contribution uncorrected. The inset shows the expanded view, showing the coercivity of the films.

Figure 6. *M* versus *H* plot of the $Sn_{0.90}Co_{0.10}O_{1.925-\delta}F_{0.075}$ film recorded at three different temperatures, 473, 523 and 573 K, indicating that the Curie temperature is above 573 K. The inset shows the temperature dependence of the magnetization of $Sn_{0.90}Co_{0.10}O_{2-\delta}$, 5 a/o, 7.5 a/o, 10.0 a/o F-doped $Sn_{0.90}Co_{0.10}O_{2-\delta-y}F_y$ films suggesting a Curie temperature (T_c) in excess of 573 K. The inset also shows the diamagnetic relationship of SnO_2 film with temperature.

$Sn_{0.90}Co_{0.10}O_{2-\delta-y}F_y$ with different F-concentration (5.0, 7.5 and 10.0 a/o) have been prepared. The *M* versus *H* behavior of these films is shown in figure 5. All the F-doped samples exhibit higher saturation magnetic moments, with a maximum value of 0.80 μ_B/Co-ion for the 7.5 a/o F-doped $Sn_{0.90}Co_{0.10}O_{2-\delta-y}F_y$ sample. This value is three times higher than the value obtained for the Co-doped SnO_2 film having no fluorine. The coercivity has also increased from 40 Oe for $Sn_{0.90}Co_{0.10}O_{2-\delta}$ to 140 Oe for $Sn_{0.90}Co_{0.10}O_{1.925-\delta}F_{0.075}$ film. The Hall measurements reveal a significant increase (nearly one order) in carrier concentration on doping with F, with a maximum carrier concentration of 2×10^{20} cm^{-3} for $Sn_{0.90}Co_{0.10}O_{1.925-\delta}F_{0.075}$ sample. The carrier concentration and the saturation magnetic moment of all the ferromagnetic samples are tabulated in table 1. The magnetic moment and carrier concentration are found to be strongly dependent on F-doping and their one-to-one correspondence strongly validates the possibility of carrier mediated ferromagnetic exchange interaction operative in $Sn_{1-x}Co_xO_{2-\delta}$ thin films. To confirm further the robust nature of ferromagnetism, *M* versus *H* data have been recorded for the $Sn_{0.90}Co_{0.10}O_{1.925-\delta}F_{0.075}$ sample at different temperatures ($T = 473, 523$ and 573 K) and are shown in figure 6. The figure clearly indicates that T_c of this film is definitely greater than 573 K. Also the temperature dependence of the magnetization measurements at $H = 650$ mT (inset of figure 6) suggests a Curie temperature greater than 573 K for $Sn_{0.90}Co_{0.10}O_{2-\delta}$ and all the $Sn_{0.90}Co_{0.10}O_{2-\delta-y}F_y$ samples. The undoped SnO_2 sample, however, shows the temperature independent diamagnetic behavior.

It is known that a greater concentration of carriers and their large mass are the two important requisites for producing a strong Ruderman–Kittel–Kasuya–Yosida type ferromagnetic interaction between the localized impurity spins [31]. The Co-doped SnO_2 thin films definitely have at least one of these special characteristics. The fact that the $Sn_{1-x}Co_xO_{2-\delta}$ with $x = 0.10$ exhibited the highest magnetization as

Table 1. Dependence of saturation magnetic moment and free carrier concentration on the cobalt concentration, x, in $Sn_{1-x}Co_xO_{2-\delta}$ and $Sn_{1-x}Co_xO_{2-\delta-y}F_y$ films.

Film composition	Carrier concentration, n ($\times 10^{19}$ cm^{-3})	Saturation magnetic moment, m_s (μ_B/Co ion)
$Sn_{0.975}Co_{0.025}O_{2-\delta}$	1.16 ± 0.05	0.04 ± 0.010
$Sn_{0.95}Co_{0.05}O_{2-\delta}$	1.85 ± 0.06	0.12 ± 0.008
$Sn_{0.925}Co_{0.075}O_{2-\delta}$	2.00 ± 0.06	0.14 ± 0.007
$Sn_{0.90}Co_{0.10}O_{2-\delta}$	2.30 ± 0.07	0.26 ± 0.013
$Sn_{0.90}Co_{0.10}O_{2-\delta-0.10}F_{0.10}$	12.01 ± 0.04	0.59 ± 0.011
$Sn_{0.90}Co_{0.10}O_{2-\delta-0.05}F_{0.05}$	18.81 ± 0.04	0.75 ± 0.011
$Sn_{0.90}Co_{0.10}O_{2-\delta-0.075}F_{0.075}$	20.65 ± 0.03	0.80 ± 0.011

well as the highest carrier concentration is clearly an indication that the carrier concentration plays a significant role in the manifestation of ferromagnetism in these films. The F-doped $Sn_{0.90}Co_{0.10}O_{2-\delta}$ samples exhibiting higher magnetic moment along with higher carrier concentration further validates carrier mediated exchange interaction as the most probable mechanism for the magnetic ordering in the $Sn_{1-x}Co_xO_{2-\delta}$ system. Present observations support a recent theoretical work by Das Sarma *et al* [32] suggesting that carrier mediated interaction may be a cause of high temperature ferromagnetism observed in oxide dilute magnetic semiconductors.

Finally it may be mentioned here that with increasing Co-concentration up to 0.10 and F-concentration up to 0.10 in SnO_2, the films do not show any appreciable reduction in optical transparency ($T \sim 75\%$ in the visible region) in the energy range of 1–3.5 eV, which is technologically very promising.

4. Conclusions

Thin films of $Sn_{1-x}Co_xO_{2-\delta}$ ($0 \leqslant x \leqslant 0.15$) and fluorine-doped $Sn_{0.90}Co_{0.10}O_{2-\delta}$ have been prepared by spray pyrolysis of constituent solutions at $450\,°C$ in three steps. The films with $0.025 \leqslant x \leqslant 0.10$ show RT ferromagnetism with associated systematic increase in carrier concentration and saturation magnetic moment. The temperature dependence of the magnetization measurements predicts a Curie temperature in excess of 573 K. Additionally, these films retain their semiconductivity and transparency, and are devoid of any detectable ferromagnetic impurities. These films exhibited an anomalous Hall effect in their magneto-transport behavior which is indicative of the carrier mediated interaction. The increase of carrier concentration (by an order) and saturation magnetic moment (nearly three fold) by F-doping in $Sn_{0.90}Co_{0.10}O_{2-\delta}$ samples further strengthened the view that the magnetic ordering in $Sn_{1-x}Co_xO_{2-\delta}$ arises due to carrier mediated exchange interaction.

Acknowledgments

References

[1] Matsumoto Y, Murakami M, Shono T, Hasegawa T, Fukumura T, Kawasaki M, Ahmet P, Chikyow T, Koshihara S and Koinuma H 2001 *Science* **291** 854
[2] Matsumoto Y, Takahashi R, Murakami M, Koida T, Fan X J, Hasegawa T, Fukumura T, Kawasaki M, Koshihara S Y and Koinuma H 2001 *Japan. J. Appl. Phys.* 2 **40** L1204
[3] Shinde S R, Ogale S B, Sarma S D, Simpson J R, Drew H D, Lofland S E, Lanci C, Buban J P, Browning N D, Kulkarni V N, Higgins J, Sharma R P, Greene R L and Venkatesan T 2003 *Phys. Rev.* B **67** 115211
[4] Griffin K A, Pakhomov A B, Wang C M, Heald S M and Krishnan K M 2005 *Phys. Rev. Lett.* **94** 157204
[5] Quilty J W, Shibata A, Son J-Y, Takubo K, Mizokawa T, Toyosaki H, Fukumura T and Kawasaki M 2006 *Phys. Rev. Lett.* **96** 027202
[6] Ueda K, Tabata H and Kawai T 2001 *Appl. Phys. Lett.* **79** 988
[7] Norton D P, Pearton S J, Hebard A F, Theodoropoulou N, Boatner L A and Wilson R G 2003 *Appl. Phys. Lett.* **82** 239
[8] Venkatesan M, Fitzgerald C B, Lunney J G and Coey J M D 2004 *Phys. Rev. Lett.* **93** 177206
Fitzgerald C B, Venkatesan M, Lunney J G, Dorneles L S and Coey J M D 2005 *Appl. Surf. Sci.* **247** 493
[9] Kobayashi M, Ishida Y, Hwang J I, Mizokawa T, Fujimori A, Mamiya K, Okamoto J, Takeda Y, Okane T, Saitoh Y, Muramatsu Y, Tanaka A, Saeki H, Tabata H and Kawai T 2005 *Phys. Rev.* B **72** 201201
[10] Yang S G, Li T, Gu B X, Du Y W, Sung H Y, Hung S T, Wong C Y and Pakhomov A B 2003 *Appl. Phys. Lett.* **83** 3746
[11] Philip J, Theodoropoulou N, Berera G and Moodera J S 2004 *Appl. Phys. Lett.* **85** 777
Philip J, Punnoose A, Kim B I, Reddy K M, Layne S, Holmes J O, Satpati B, Leclair P R, Santos T S and Moodera J S 2006 *Nat. Mater.* **5** 298
[12] He J, Xu S, Yoo Y K, Xue Q, Lee H-C, Cheng S, Xiang X-D, Dionne G F and Takeuchi I 2005 *Appl. Phys. Lett.* **86** 052503
Yu Z G, He J, Xu S, Xue Q, van't Erve O M J, Jonker B T, Marcus M A, Yoo Y K, Cheng S and Xiang X 2006 *Phys. Rev.* B **74** 165321
[13] Hong N H, Sakai J, Huong N T and Brize V 2005 *Appl. Phys. Lett.* **87** 102505
[14] Peleckis G, Wang X L and Dou S X 2006 *Appl. Phys. Lett.* **88** 132507
[15] Ogale S B, Choudhary R J, Buban J P, Lofland S E, Shinde S R, Kale S N, Kulkarni V N, Higgins J, Lanci C, Simpson J R, Browning N D, Das Sarma S, Drew H D, Greene R L and Venkatesan T 2003 *Phys. Rev. Lett.* **91** 077205
[16] Fitzgerald C B, Venkatesan M, Douvalis A P, Huber S, Coey J M D and Bakas T 2004 *J. Appl. Phys.* **95** 7390
[17] Punnoose A, Hays J, Gopal V and Shutthanandan V 2004 *Appl. Phys. Lett.* **85** 1559
Hays J, Punnoose A, Baldner R, Engelhard M H, Peloquin J and Reddy K M 2005 *Phys. Rev.* B **72** 075203
[18] Fitzgerald C B, Venkatesan M, Dorneles L S, Gunning R, Stamenov P, Coey J M D, Stampe P A, Kennedy R J, Moreira E C and Sias U S 2006 *Phys. Rev.* B **74** 115307
[19] Gopinadhan K, Pandya D K, Kashyap S C and Chaudhary S 2006 *J. Appl. Phys.* **99** 126106
Gopinadhan K, Kashyap S C, Pandya D K and Chaudhary S 2007 *J. Appl. Phys.* **102** 113513
Gopinadhan K, Pandya D K, Kashyap S C and Chaudhary S 2007 *J. Phys.: Condens. Matter* **19** 016216
[20] Wang X L, Dai Z X and Zeng Z 2008 *J. Phys.: Condens. Matter* **20** 045214
[21] Jousse D 1985 *Phys. Rev.* B **31** 5335
[22] JCPDS-International Centre for Diffraction Data 2002, File #-72-1147. Ref. Baur W H 1956 *Acta Crystallogr.* **9** 515
[23] Lide D R 2005–2006 *CRC Handbook of Chemistry and Physics* 87th edn, ed D R Lide (London: Taylor and Francis) pp 12–11
[24] Rachinger W A 1948 *J. Sci. Instrum.* **25** 254
[25] Kilic C and Zunger A 2002 *Phys. Rev. Lett.* **88** 095501
[26] Yoshikawa H, Hayashida K, Kozuka Y, Horiguchi A, Awaga K, Bandow S and Iijima S 2004 *Appl. Phys. Lett.* **85** 5287
[27] Shinde S R, Ogale S B, Higgins J S, Zheng H, Millis A J, Kulkarni V N, Ramesh R, Greene R L and Venkatesan T 2004 *Phys. Rev. Lett.* **92** 166601
[28] Shanthi E, Dutta V, Banerjee A and Chopra K L 1980 *J. Appl. Phys.* **51** 6243
[29] Chopra K L, Major S and Pandya D K 1983 *Thin Solid Films* **102** 1
[30] Gupta A, Pandya D K and Kashyap S C 2004 *Japan. J. Appl. Phys.* 2 **43** L1592
[31] Dietl T, Haury A and d'Aubigne Y M 1997 *Phys. Rev.* B **55** R3347
[32] Calderon M J and Das Sarma S 2007 *Ann. Phys.* **322** 2618